Noise performance of surface coils for magnetic resonance imaging at 1.5 T

Cecil E. Hayes
Applied Science Laboratory, Medical Systems Group, General Electric Co., Milwaukee, Wisconsin 53201
Leon Axel
Department of Radiology, Hospital of the University of Pennsylvania, Philadelphia, Pennsylvania 19104

(Received 4 January 1985; accepted for publication 11 April 1985)

In this paper we analyze the signal-to-noise ratio (SNR) for surface coil magnetic resonance imaging at 1.5 T. We have applied the treatment of Hoult and Lauterbur to determine the factors that most affect coil performance. We have imaged lossy phantoms with 8-, 10-, and 14-cm-diam circular surface coils and compared the results to body and head coil images. Surface coils can improve SNR by a factor of 4 or more for regions close to the surface. Surface coils are effective for regions up to 6 cm deep in the head and about 12 cm deep in the body. Nonuniformity of image intensity is a necessary requirement for improved SNR in surface coils. Coil losses make only a small contribution to image noise compared to tissue losses at 1.5 T. Surface coils need not be placed in close contact with the patient at 1.5 T.

I. INTRODUCTION

Magnetic resonance imaging (MRI) with surface coils is a rapidly developing technique [1–6] which provides improved image quality for relatively superficial structures in the body. The chief advantage of using a surface coil arises from the higher signal-to-noise ratio (SNR) possible compared to using a head or body coil. The better SNR from a surface coil can be used to decrease imaging time, particularly at low magnetic field strengths, or to decrease pixel size and thereby increase the resolution of structural details. The chief disadvantage of surface-coil imaging is the rapid falloff in signal strength with distance from the coil. Unfortunately, this nonuniform spatial response is a necessary condition for the improved SNR in surface coils.

The above cited studies were primarily concerned with demonstrating the improved clinical images possible with surface coils and with discussing the diagnostic potential of surface-coil imaging of various parts of the body. They are largely qualitative in nature. In this report, we discuss the factors affecting the noise performance of surface coils, describe some measurement techniques useful in analyzing surface coils, and give quantitative results from some simple imaging experiments performed in a 1.5-T magnetic field.

II. NOISE IN SURFACE COILS

In 1979, Hoult and Lauterbur[7] first discussed the principal sources of noise in magnetic resonance imaging. They applied the fluctuation–dissipation theorem, which states that any dissipative medium generates thermally activated random fluctuations, which can be detected as noise. There are two dissipative elements which are the principal noise sources in MRI. The first is the series resistance of the receiver coil r_{coil} due to conductive losses of the wire. The second is the magnetically induced eddy current losses in the sample or patient. This loss mechanism can be represented by an equivalent series resistor r_{sample} to account for the loading effect on the receiver coil by the sample. The expression for SNR is[7]

$$\text{SNR} \propto (\omega^2 B_1)/\sqrt{r_{\text{coil}} + r_{\text{sample}}}, \tag{1}$$

where ω is the Larmor frequency. The B_1 factor arises from the reciprocity theorem,[8] which states that the signal induced in a coil by a precessing nucleus will be proportional to the magnetic field B_1 produced at the nucleus by a unit current in the coil. Hoult and Lauterbur derived an expression for r_{sample} by calculating the energy dissipated in a sphere of radius b with electrical conductivity σ subjected to a homogeneous rf field B_1. They found[7]

$$r_{\text{sample}} \propto \sigma\omega^2 B_1^2 b^5. \tag{2}$$

The strong dependence of r_{sample} on Larmor frequency ω and sample size b results in tissue losses becoming the dominant noise source when imaging bodies or heads at high fields. We find that, for whole-body imaging at 1.5 T, r_{sample} is typically six or more times as large as r_{coil}. Neglecting r_{coil} and substituting Eq. (2) into Eq. (1) gives

$$\text{SNR} \propto (\omega/\sqrt{\sigma b^5}). \tag{3}$$

Note that the B_1 factor, which depends on the coil geometry, has dropped out. The SNR for a fixed voxel size decreases as the tissue volume in the receiver coil increases.

Equation (1) also applies to surface-coil imaging where the inhomogeneity of the receiver coil sensitivity B_1 imparts the only spatial dependence to the SNR. That is, we assume all the nuclei are uniformly stimulated by a larger transmitter coil, which produces a homogeneous rf field. For simplicity, we consider a single turn circular receiver coil having radius a and lying in the $x = 0$ plane at the surface of the sample. B_1 has a simple expression when evaluated on the x axis. In this case, the signal is given by

$$\text{Signal} \propto \omega^2 B_1(x,a) \propto \frac{\omega_2}{a[1 + (x^2/a^2)]^{3/2}}. \tag{4}$$

Note that, for $x = 0$, the signal for a fixed voxel size increases as coil radius decreases. Equation (2) no longer applies for r_{sample} of a surface coil, where B_1 is not uniform. The $B_1^2\, b^5$ factor in Eq. (2) must be replaced by a much more complicated function of coil geometry and sample geometry. The rapid falloff of coil sensitivity B_1 with distance implies that randomly fluctuating currents in the tissue far from the coil produce little noise in the receiver coil. Hence those portions

 0094-2405/85/050604-04$01.20

of the sample closest to the coil contribute the most to r_{sample}. The effective volume of tissue that loads the coil is essentially determined by the coil radius a, provided that the sample dimensions are large compared to the coil. Hence we expect for a surface coil,

$$r_{sample} \propto \sigma\omega^2 f(a), \tag{5}$$

where $f(a)$ should be a rapidly increasing function of a. For the coil sizes useful in surface imaging, we find r_{sample} is nine or more times as large as r_{coil}. Hence substituting Eqs. (4) and (5) into Eq. (1) and neglecting r_{coil}, we obtain

$$\text{SNR} \propto (\omega/a\sqrt{\sigma f(a)})[1 + (x^2/a^2)]^{-3/2}. \tag{6}$$

The first factor suggests that the SNR at the surface ($x = 0$) increases rapidly as the coil radius a is decreased. The second factor demonstrates that the radius a is the scale factor which determines how rapidly the SNR rolls off with distance into the sample. Hence, in contrast with Eq. (3) for head or body imaging, the SNR for surface imaging depends little on the total tissue volume and greatly on coil geometry.

III. METHODS

The most common quantity for characterizing a resonant circuit is the quality factor Q. Q is defined as the ratio of the peak magnetic energy stored by the coil to the average energy dissipated per radian by the coil. High Q implies low losses. The Q is numerically equal to the resonant frequency ω divided by the 3-dB bandwidth $\Delta\omega$ or the inductive impedance ωL divided by the equivalent series resistance r. Equating the two expressions for Q leads to the relationship $r = L\Delta\omega$. Hence a relatively small valued radio-frequency resistance can be accurately deduced from measurements of inductance and bandwidth. The quantity r_{coil} is proportional to the 3-dB bandwidth when the coil is empty and r_{sample} is proportional to the increase in bandwidth when the sample is added. With this operational definition r_{coil} includes losses due to matching network, cables, clipping diodes, and coil resistance, but not the loading due to the preamplifier. The preamplifier is not connected during Q measurements. The Q can be measured with a radio-frequency signal generator, an oscilloscope, a frequency counter, and two inductive loops. The inductive loops, which are small compared to the coil under test, are placed on opposite sides of the coil. One loop, driven by the signal generator, excites the coil's resonance and the other, connected to the scope, monitors the coil's response. For high-Q coils, the two loops must be loosely coupled to the coil to prevent loading of the coil by either the output impedance of the generator or the input impedance of the scope. The resonant frequency and the low- and high-frequency -3-dB points can be determined by manually tuning the signal generator. We obtained the same results more quickly by using the inductance loops with a spectrum analyzer and tracking generator in place of the scope and signal generator.

In the experiments described below, the SNR was obtained by imaging homogeneous phantoms containing distilled water doped with NaCl and $CuSO_4$. The $CuSO_4$ concentration was about 0.01 M, which gave a convenient T_1 spin-lattice relaxation time. Our simple "head" phantom consisted of a 1-gal plastic bottle with enough NaCl added to make it load a head coil to the same degree as a typical human head. The bottle was oriented on its side with its longer dimension parallel to the main magnetic field. The second phantom was a 21-cm square flat-bottomed plastic container with 11 cm of water in it. In use, this phantom was centered on top of the surface coil. The NaCl concentration was adjusted so that the phantom's loading on the surface coil equalled that caused by placing the coil against a human abdomen. In both cases, the NaCl concentration was approximately 0.034 M.

In our surface coil imaging experiments, the nuclei are excited by transmitting with the body coil. Thus all the nuclei are subjected to essentially the same flip angles, provided no significant currents are induced in the surface coil during the transmit pulse. The induced current can be limited by adding clipping diodes to the surface coil. Also, the transmit and receive coils can be decoupled by positioning their axes orthogonally. Decoupling is useful also during the receive mode. Otherwise, the body coil can pick up noise originating in parts of the body far from the surface coil and couple it into the surface coil.

The three different surface coils used below were made by wrapping one turn of copper foil strip, 1.27 cm wide, on short sections of 8-, 10-, and 14-cm-diam acrylic tubing. Each coil was tuned and impedance matched to give a 50-Ω real source impedance when loaded by the phantom. Thus the preamplifier exhibited the same noise figure for all the experiments. The receiver gain was also kept fixed so that the same noise level appeared in all images. For each coil, the same spin-echo pulse sequence with a repetition time of 300 ms was used to make an image which included the axis of the coil. The signal amplitude versus depth along the coil axis was read directly from the image printout. The resulting SNR's were expressed as relative values only, since some partial saturation occurred for the T_1 and repetition rate used. Higher absolute SNR values could be obtained with less $CuSO_4$ doping and very long repetition time.

IV. OBSERVATIONS

Measurements were made to answer the following questions about surface coil noise performance: How important are coil losses compared to tissue losses? How well does the analysis given above apply? How do surface coils perform compared to head or body coils? Must the surface coil be placed flush against the sample? We will address these issues in the order given above.

Table I gives values of Q for three loading conditions for each of the three surface-coil diameters employed. Q_{empty} was measured with no sample present. Q_{head} was obtained

TABLE I. Coil quality factors and coil noise contribution.

Coil diameter (cm)	Q_{empty}	Q_{head}	Q_{square}	Coil noise (%)
8	274	44	38	7.2
10	298	33	32	5.5
14	245	26	18	3.7

with the coil against the side of the head phantom, and Q_{square}, with the coil centered against the bottom of the square phantom. The fifth column gives noise attributed to the coil losses expressed as a percentage of total observed noise. This factor is given by

$$\frac{\text{Coil noise}}{\text{Total noise}} = \frac{\sqrt{r_{\text{coil}} + r_{\text{sample}}} - \sqrt{r_{\text{sample}}}}{\sqrt{r_{\text{coil}} + r_{\text{sample}}}}$$

$$= 1 - \sqrt{1 - (Q_{\text{square}}/Q_{\text{empty}})},$$

where the square phantom was used as the sample. The coil noise contribution decreases as the surface coil radius increases and is essentially negligible for all three coil sizes at this frequency of operation (63.88 MHz). The variations in Q_{empty} for the three coil sizes arise primarily from variations in the losses of auxiliary components such as the clipping diodes. Unencumbered coils had empty Q's of approximately 470.

There was a possibility that some of the loading of the phantom was due to dielectric losses induced by stray electric fields coupling the coil and sample. The relative magnitude of the stray electric fields can be determined by placing a lossless phantom (distilled water) next to the surface coil and observing the decrease in resonant frequency. The high dielectric constant of water increases the effective stray capacitance. Adding NaCl to the water produces an inductive coupling effect which opposes the capacitive frequency shift. In a series of experiments with a fixed coil size, we were able to vary the stray electric fields (as evidenced by the resonant frequency shifts due to the distilled water phantom) without changing the rf magnetic fields. The incremental increase in bandwidth caused by the lossy phantom did not depend on the variation in stray electric fields. Hence we concluded that dielectric losses did not contribute significantly to the surface coil losses at 64 MHz.

Figure 1 gives plots of the relative SNR along the surface coil axis versus the depth measured from the surface of the head phantom for the three coil diameters used. Also included for comparison is the SNR versus depth for a head coil used as both transmitter and receiver coil. The functional dependence of the SNR on depth is well described by the second factor in Eq. (6), using the known values of radius a, provided x is taken as the depth plus an offset Δx. Here, $\Delta x \simeq 0.6$ cm, which corresponds to the distance between the center of the coil and water interface. The rapid variation of SNR at the surface for the three different radii demonstrates the expected inverse radial dependence of the first factor in Eq. (6).

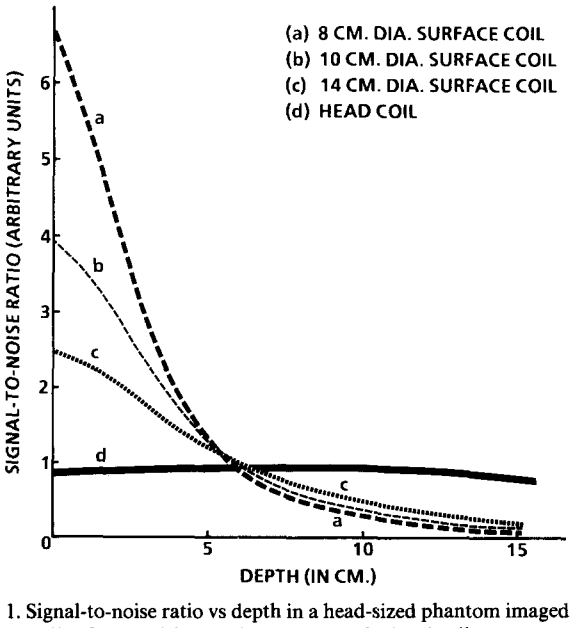

FIG. 1. Signal-to-noise ratio vs depth in a head-sized phantom imaged with surface coils of three different diameters and the head coil.

A surprising feature in Fig. 1 is that the SNR's for all three surface coils fall below that of the head coil at nearly the same depth. For depths greater than 6 cm, the head coil will probably outperform any surface coil. For depths less than 6 cm in the head, the choice of surface coil radius is primarily determined by the desired field of view extending parallel to the surface. Increasing coil radius increases the useful imaging volume but decreases the SNR. For a region 2 cm below the surface, the 8-cm-diam surface coil SNR is 4.7 times better than that of the head coil. Resolution could be enhanced by reducing the voxel size by the same factor while still retaining the same SNR as provided by the head coil. Surface coils perform even better compared to imaging the torso with a body coil. As expected from Eq. (3), the SNR in a whole-body image decreases, due to the increased losses in the larger sample. On the other hand, the SNR for a surface coil should be essentially unaffected by the larger tissue volume present. For example, when we imaged a large lossy phantom with the 14-cm-diam surface coil, the SNR at the surface was 5.6 times better than that produced by the body coil. The SNR of the surface coil dropped below that of the body coil at a depth of 11.4 cm. Larger surface coils should outperform the body coil at somewhat greater depths. Patient losses were also the dominant noise source for the head and body images. Hence the surface coil performance relative to head and body imaging would be little changed by reduced coil losses but could be influenced by the size and shape of the head and body coils. Smaller head or body coils would give better SNR's at the expense of poorer uniformity of image intensity.

The effect on SNR of withdrawing the 14-cm-diam surface coil from the bottom surface of the square phantom is demonstrated in Fig. 2. Images were taken for various separations between the top of the coil and the bottom of the phantom. The coil was retuned and matched to 50 Ω for each new separation. The SNR values plotted were taken from two regions fixed in the phantom. The superficial region was located on the coil axis immediately above the bottom surface of the phantom. The interior region was located on the coil axis, 7 cm above the bottom surface of the phantom. Both regions exhibit a nearly constant SNR for separations less than 4 cm. At 5-cm separation, both SNR's are about 90% of their peak values. An explanation of this behavior lies in the fact that the lossy sample material produces both the signal and the bulk of the noise when the coil is tightly coupled to the sample. Withdrawing the coil decreases the signal strength, as would be predicted by increasing x in Eq. (4). The constant SNR therefore implies that r_{sample} must also decrease as separation increases. The geometric factor

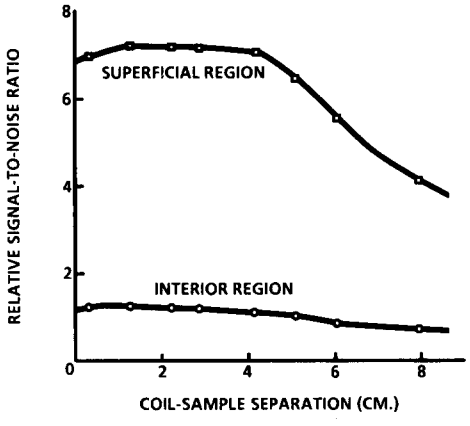

FIG. 2. Signal-to-noise ratio vs the distance by which a 14-cm-diam surface coil is displaced below the bottom of a lossy phantom. The superficial region is located adjacent to the bottom of the phantom and the interior region is located 7 cm above the bottom.

$f(a)$ in Eq. (5) must decrease rapidly as separation increases. At larger separations, the signal decreases asymptotically to zero, but the noise is bounded by the coil losses r_{coil}, and so the SNR decreases to zero.

V. CONCLUSIONS

Surface coil imaging can produce substantially higher signal-to-noise ratios for regions near the surface than can conventional head and body imaging. Surface coils are effective for depths up to about 6 cm in heads and about twice that in bodies. Surface coils produce better SNR's because the coil sensitivity factor B_1 is higher for smaller coils and because less noise is detected from distant parts of the sample. Nonuniformity of image intensity is therefore a necessary requirement for reduced noise detection. At high fields, tissue losses are the dominant source of noise. Thus coil losses make only a small contribution to the total noise and coils need not be placed in close contact with the patient.

ACKNOWLEDGMENTS

The authors are grateful to Dr. W. A. Edelstein and Dr. J. F. Schenck for many useful discussions of surface-coil technology. Leon Axel is an Established Investigator of the American Heart Association and is supported in part by funds from the Southeast Pennsylvania Chapter.

[1]M. L. Bernardo, A. J. Cohen, and P. C. Lauterbur, in *IEEE Proceedings of the International Workshop on Physics and Engineering in Medical Imaging* (IEEE, New York, 1982), pp. 277–84.
[2]S. J. El Yousef, R. J. Alfidi, R. H. Duchesneau, C. A. Hubay, J. R. Haaga, P. J. Bryan, J. P. LiPuma, and A. E. Ament, J. Comput. Assist. Tomogr. **7**, 215 (1983).
[3]L. Axel, J. Comput. Assist. Tomogr. **8**, 381 (1984).
[4]J. F. Schenck, H. R. Hart, T. H. Foster, W. A. Edelstein, P. A. Bottomley, R. W. Redington, C. J. Hardy, R. A. Zimmerman, and L. T. Bilaniuk, Am. J. Neuroradiol. **6**, 193 (1985).
[5]W. A. Edelstein, J. F. Schenck, H. R. Hart, C. J. Hardy, T. H. Foster, and P. A. Bottomley, J. Am. Med. Soc. **253**, 828 (1985).
[6]J. F. Schenck, T. H. Foster, J. L. Henkes, W. J. Adaams, C. E. Hayes, H. R. Hart, W. A. Edelstein, P. A. Bottomley, and F. W. Wehrli, Am. J. Neuroradiol. **6**, 181 (1985).
[7]D. I. Hoult and P. C. Lauterbur, J. Magn. Reson. **34**, 425 (1979).
[8]D. I. Hoult and R. E. Richards, J. Magn. Reson. **24**, 71 (1976).